Am J Nucl Med Mol Imaging 2015;5(5):504-514
www.ajnmmi.us /ISSN:2160-8407/ajnmmi0010658

Original Article

Quantitative differences in [^{18}F] NaF PET/CT: TOF versus non-TOF measurements

Jorge D Oldan[1], Timothy G Turkington[1,3], Kingshuk Choudhury[2], Bennett B Chin[1,3]

[1]*Department of Radiology, Division of Nuclear Medicine, Duke University Medical Center, Durham, NC, USA;* [2]*Department of Radiology, Duke University Medical Center, Durham, NC, USA;* [3]*Duke University Graduate School of Medical Physics, Duke University, Durham, NC, USA*

Received May 25, 2015; Accepted July 6, 2015; Epub October 12, 2015; Published October 15, 2015

Abstract: [^{18}F] sodium fluoride (NaF) PET/CT is a current, clinically relevant method to assess bone metastases. Time-of-flight (TOF) PET provides better statistical data quality, which can improve either lower image noise or improve resolution, or both, depending on the image reconstruction. Improved resolution can improve quantitative measurements of standardized uptake value (SUV) in small structures. These quantitative differences may be important in both clinical interpretation and multicenter clinical trials where quantification is integral to assessing response to therapy. The purpose of this study is to determine if and by how much SUV quantitatively differs between TOF and conventional non-TOF reconstructions in [^{18}F] NaF PET/CT. SUV measurements (mean and maximum) were compared in TOF and non-TOF [^{18}F] NaF PET-CT reconstructions for 47 prostate cancer patients in normal regions including: soft tissue (n=282 total regions; liver, aorta, posterior abdominal fat, bladder, brain, and paraspinal muscles), and osseous structures (n=188; T12 vertebral body, femoral diaphyseal cortex, femoral head, and lateral rib). Comparisons were also made for benign degenerative changes (n=281) and metastases (n=159). TOF and non-TOF SUVs were assessed with paired t-test and linear correlations. Normal soft tissue showed lower SUV_{mean} for TOF compared to non-TOF in liver, brain, and adipose. All osseous structures showed higher SUV_{mean} for TOF compared to non-TOF including normal regions, degenerative joint disease, and metastases. For all metastatic lesions, the average SUV_{mean} increased by 2.5%, and in degenerative joint disease it increased by 3.5% on TOF reconstructions. Smaller lesion size was a significant factor influencing this increase in SUV_{mean}. TOF SUV_{mean} values are higher in osseous structures and lower in background soft tissue structures. While these differences are statistically significant, the magnitudes of these changes are relatively modest. Smaller osseous lesions may have higher contrast and higher SUV_{mean} values with TOF reconstruction compared to non-TOF reconstructions. The differences in TOF vs. non-TOF images should be considered when evaluating response to therapy and in the design of multi-center clinical trials.

Keywords: Sodium fluoride, prostate cancer, time of flight, positron emission tomography, PET/CT, quantification

Introduction

Combined [^{18}F] sodium fluoride positron emission tomography with CT imaging ([^{18}F] NaF PET/CT) is clinically used to assess for the presence of bone metastases. Overall, [^{18}F] NaF PET/CT has demonstrated higher accuracy in detection of bone metastases compared to planar ^{99m}Tc MDP bone scintigraphy [1-3]. The higher contrast of tomography and the high spatial resolution of PET both contribute to improved sensitivity and the ability to correlate with CT findings improves specificity.

Another potential advantage of PET/CT is more accurate quantification due to attenuation correction. Quantification of metabolically active bone or metastatic volume may be important in determining response to therapy or prognosis [4]. Quantification is potentially useful if measurements are highly reproducible; thus, identifying which variables influence measurements and how much they may influence measurements are important factors to consider in attempting to reduce the variability of measurements. This may be particularly relevant to multicenter clinical trials where measurements may be used to determine the effectiveness of a treatment.

Time-of-flight (TOF) data acquisition is an improvement in PET, which at a given image

noise level, improves image contrast recovery [5, 6]. This can result in faster and more uniform convergence with iterative reconstruction, but this may also affect image quantification in [18F] NaF PET/CT. The TOF technique improves activity localization by more accurately identifying an annihilation event along a line of response using the arrival time ("time of flight"). In early clinical observer 2-deoxy-2-[18F] fluoro-D-glucose ([18F] FDG PET) studies, it increased contrast recovery, improved image quality, and also improved quantitative accuracy and precision [7-11].

For [18F] NaF PET/CT, the improvement in contrast recovery with TOF reconstruction could be seen clinically as higher SUV in high uptake structures of bone; this difference is expected to be greatest in smaller lesions where the effect of contrast recovery is greatest. Smaller lesions may also be associated with a lower SUV due to the partial volume effect; smaller SUV values could, therefore, also be associated with a difference in TOF compared to non-TOF reconstruction measurements. An improvement in contrast recovery could also be seen in larger patients due to a lower scatter fraction from adjacent soft tissues as seen with [18F] FDG PET [7, 8]. Although we hypothesize similar relationships with [18F] NaF PET/CT, the radiotracer biodistribution and uptake levels are quite different compared with FDG. This is relevant to both clinical interpretations, and our investigations which quantifythe extent of bone metastases by [18F] NaF PET/CT using a threshold method based on the SUV [12]. The purpose of this study is to determine if quantitative differences are present in TOF compared to non-TOF [18F] NaF PET/CT, and to determine the quantitative magnitude of the differences. A secondary exploratory goal is to determine if scan specific factors (metastatic tumor location, lesion size or volume, patient weight, and standardized uptake mean value) may be associated with these differences.

Materials and methods

Subjects

This retrospective study was reviewed and approved by our institutional review board (IRB). Patients with prostate cancer referred for [18F] NaF PET/CT (n=47) had studies retrieved by an independent data analyst prior to blinded interpretation and analysis by a board-certified nuclear medicine physician. The median patient weight was 90 kg (mean=91.4; range=60-128 kg). Studies were first examined to ensure that both time-of-flight and non-time-of-flight images were available, and that no dose infiltration was apparent as determined by absence of axillary lymph node uptake in the extremity of injection.

[18F] NaF PET/CT imaging

All patients were examined on a dedicated time-of-flight-capable PET/CT system with 64 CT detector rows (Discovery 690, General Electric, Milwaukee, WI, USA). Patients received approximately 10 mCi (10.2±0.37 mCi; 377.4±13.7 MBq) of [18F] NaF. The mean uptake phase was 65.2 minutes (SD 10.5 minutes, range 57-107 minutes). All patients were instructed to void prior to imaging. A non-contrast CT was performed using a protocol with the following parameters: tube current of 10-300 mA determined by an automated algorithm based on the planar view to achieve a noise index of 18, 140 kVp, and pitch 0.984. The CT axial images were reconstructed in a 512×512 matrix of 50 cm FOV, with a thickness of 3.75 mm and 3.27 mm center-to-center spacing. PET was performed with 3D acquisition at 2 minutes per 7.5-cm bed position from the elbows (with elbows held above the head) to below the knees, with 11-12 bed positions total. TOF images used an iterative reconstruction method (GE, OSEM), 2 iterations, 16 subsets, and Gaussian post-reconstruction filtering with a 6.4 mm filter width. The non-TOF images used this iterative reconstruction method with 2 iterations and 24 subsets, with the same Gaussian post-reconstruction filtering. The smaller number of subset iterations in the TOF reconstructions were performed to visually match the noise properties of the non-TOF reconstructions, with TOF images being slightly less noisy by visual interpretation [13]. In all cases, a non-contrast CT was used for PET attenuation correction, and additional corrections for scatter, random events, and dead time were performed with a matrix size of 128×128, also covering a 50-cm FOV with the OSEM algorithm.

Data analysis

Reconstructed images were transferred from the scanner workstation offline to a data analysis MIM vista workstation (MIM software,

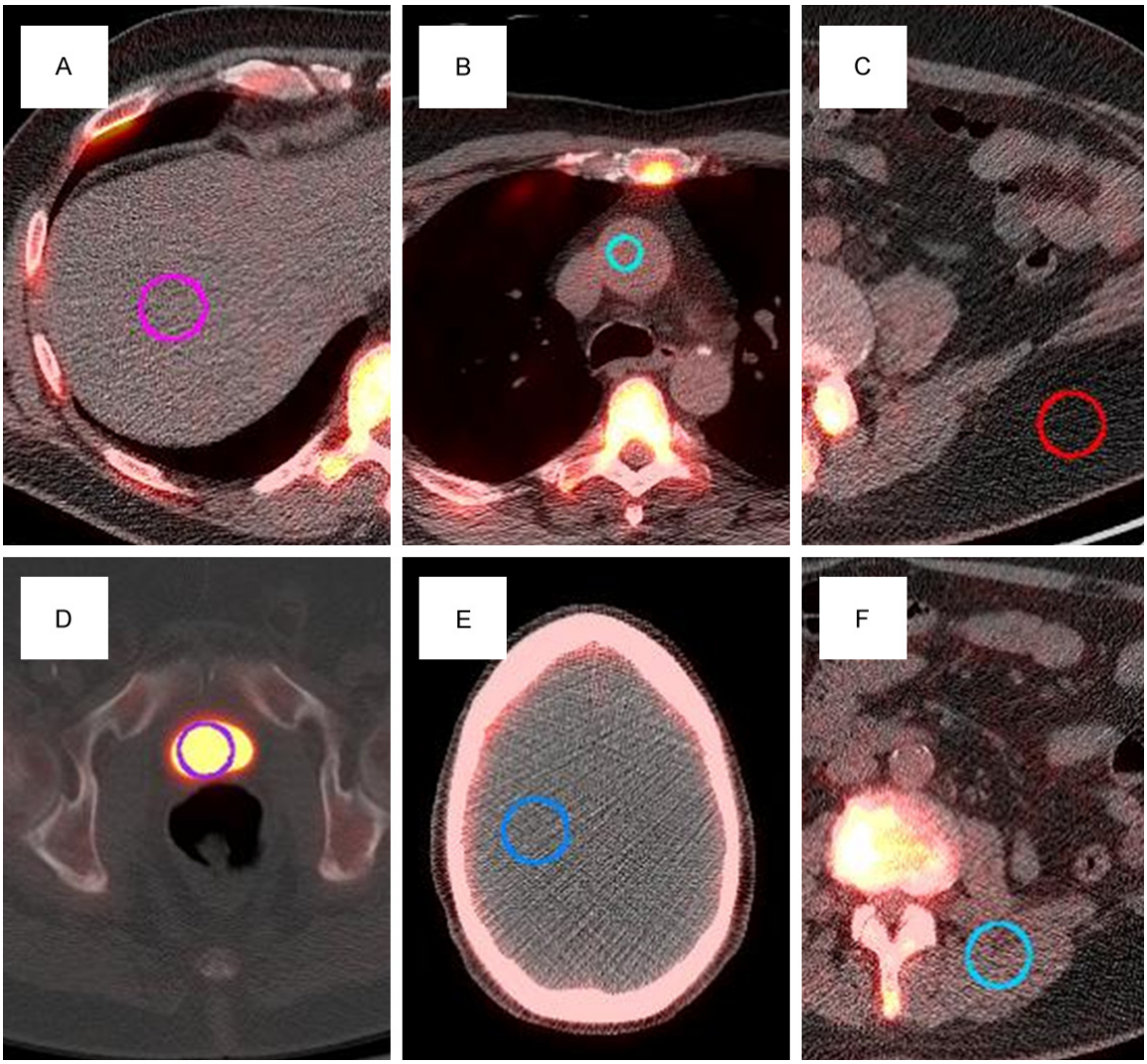

Figure 1. Typical ROIs for (A) liver, (B) aorta, (C) fat, (D) bladder, (E) brain, and (F) paraspinal muscles.

Cleveland, OH) for region of interest (ROI) analysis. ROIs were drawn using a circular ROI tool over 6 contiguous axial slices when possible. Typical location and size of some soft tissue ROI examples shown in **Figure 1**. Smaller ROIs were used for smaller organs with the CT used as a guide to determine boundaries. A smaller ROI in the femoral head was drawn at the point of maximum thickness by CT. The T12 vertebral body ROI was chosen to accommodate as much of the T12 vertebral body as possible but to avoid the endplates, as they could contain degenerative changes. In the ascending aorta and aortic arch, a smaller 15 mm diameter circular ROI was chosen to avoid the calcification at the margins of the arteries, which has been known to take up sodium fluoride [14-15]. Smaller circular ROI were used in the ribs (in the mid-axillary line of the right 6th rib, or adjacent rib if involved by metastatic disease).

Degenerative changes and metastatic lesions were then segmented using a threshold-based model with the boundaries defined at 50% of SUV maximum, similar to previous reports using thresholds of 40-50% [16-18]. After a lesion was identified, the lesion boundaries were automatically determined by a computer thresholding feature (MIM software) to include all voxels greater than or equal to 50% of the maximum SUV of a lesion. These ROI boundaries were saved and superimposed on both sets of images to enable paired comparisons between TOF and non-TOF reconstructions. To

Table 1. Average SUV_{mean} in TOF and non-TOF reconstructions (differences significant if p<0.00417)

Organ	*TOF*	*TOF sd*	*Non-TOF*	*Non-TOF sd*	*p-value*	*Higher value*
Liver	0.49	0.13	0.65	0.17	<0.0001	Non-TOF
Aorta	1.21	0.24	1.24	0.26	0.0056	NS
Bladder	41.88	24.13	41.62	24.32	0.0032	TOF
Fat	0.18	0.05	0.20	0.05	<0.0001	Non-TOF
Brain	0.15	0.04	0.21	0.08	<0.0001	Non-TOF
Paraspinal muscles	0.70	0.11	0.68	0.11	0.0065	NS
T12	6.80	1.44	6.71	1.40	0.0001	TOF
Cortex	1.68	0.65	1.58	0.64	<0.0001	TOF
Femoral head	2.31	0.95	2.19	0.87	<0.0001	TOF
Rib	3.46	0.81	3.30	0.79	<0.0001	TOF
DJD (n=281)	11.07	3.81	10.71	3.77	<0.0001	TOF
Metastases (n=159)	16.29	12.99	16.11	13.18	0.0001	TOF

Table 2. Average SUV_{max} in TOF and non-TOF reconstructions (differences considered significant for p<0.00417)

Organ	*TOF*	*TOF sd*	*Non-TOF*	*Non-TOF sd*	*p-value*	*Higher value*
Liver	0.84	0.23	1.15	0.38	<0.0001	Non-TOF
Aorta	1.61	0.33	1.78	0.44	0.0004	Non-TOF
Bladder	58.48	37.69	58.34	37.72	0.5188	NS
Fat	0.41	0.14	0.46	0.15	0.0007	Non-TOF
Brain	0.34	0.12	0.44	0.13	<0.0001	Non-TOF
Paraspinal muscles	1.32	0.35	1.33	0.31	0.6923	NS
T12	9.32	1.82	9.55	1.91	0.0064	NS
Cortex	2.21	0.89	2.14	0.88	0.0178	NS
Femoral head	3.53	1.55	3.39	1.42	0.0043	NS
Rib	4.38	1.05	4.33	1.02	0.2264	NS
DJD (n=281)	16.65	5.66	16.27	5.70	<0.0001	TOF
Metastases (n=159)	23.95	18.87	23.81	19.20	0.1042	NS

enable comparisons of exactly the same regions, the TOF SUV_{max} was chosen to define the boundaries for the volumes for TOF and non-TOF reconstructions. For osseous lesions, 44 patients had visible degenerative disease with a total of 281 lesions, and 24 patients had a total of 159 metastases. Both the mean and maximum standardized uptake values corrected for body weight are reported. Linear correlations with weight are reported as well. To calculate the percentage difference, the TOF values were expressed as a percentage difference from non-TOF values as follows: % difference = (TOF SUV- non-TOF SUV)/(non-TOF SUV) × 100%. Because SUV_{max} may be more affected by image noise, we report SUV_{mean} comparisons.

Statistical analysis

To compare TOF and non-TOF measurements, two-sample paired t-tests were performed. To achieve an alpha of 0.05, a conservative multiple comparisons correction of Bonferroni was applied (n=12 different ROIs compared in each patient), and a significant difference was defined at the p<0.00417 level.

To assess the relationship between these differences in SUV_{mean} and scan specific factors, we performed a secondary analysis, with the proposed multivariate model for differences of the form:

$$d_{ij} = \mu + b_i + T_{ij} + \beta_1 \log(V_{ij}) + \beta_2 W_i + \beta_3 \log(S_{ij}) + \log(S_{ij})\varepsilon_{ii} \quad (1)$$

The response is the difference in mean SUV within the ROI between TOF and non-TOF based reconstructions, d_{ij} = mean SUV(TOF)-mean SUV (non-TOF) for the *j*-th lesion in the *i*-th subject. Model (1) above explains this difference in terms of a baseline average response μ, where baseline corresponds to a metastatic lesion of size 2.5 cm^3 and mean SUV of 10 in the rib, for a subject weighing 92 kg. The choice of baseline values of the covariates represents typical values in the study population: 'Rib' is the most common lesion location, 2.5 cm^3 is the mean size of metastatic lesions, 10 is the median SUV and 92 kg is the mean body weight. The next term is a subject specific effect b_i, which also potentially captures differences in scan parameters and is assumed to be a random variable with a Gaussian distribution with zero mean and SD σ_b. The effect of tissue type is captured by the term T_{ij}. The coefficient β_1 captures the effect of lesion volume V_{ij} on the difference. The lesion volume was log transformed to spread out the distribution, which is clustered at the small end. The coefficient β_2 captures the effect of body weight W_i on the difference. The coefficient β_3 captures

Table 3. Mean differences of TOF measurements SUV_{mean} and SUV_{max}. Results are expressed in terms of mean percentage difference (% non-TOF) and in absolute SUV values (SUV_{mean} and SUV_{max})

Organ	Difference SUV_{mean} (TOF-non-TOF)		Difference SUV_{max} (TOF-non-TOF)	
	% non-TOF	SUV_{mean}	% non-TOF	SUV_{max}
Liver	-23.03	-0.15	-38.39	-0.31
Aorta	-2.42	-0.04	-9.55	-0.16
Bladder	1.18	0.26	0.46	0.14
Fat	-10.83	-0.02	-13.06	-0.05
Brain	-27.74	-0.06	-30.94	-0.09
T12	1.26	0.09	-2.55	-0.23
Cortex	6.90	0.10	2.98	0.07
Femoral head	4.72	0.12	2.88	0.15
Paraspinal muscles	2.69	0.02	-2.14	-0.01
Rib	5.32	0.16	0.87	0.05
Degenerative changes	3.72	0.36	2.71	0.38
Metastases	2.53	0.18	1.96	0.14

the effect lesion mean SUV S_{ij} on the difference. The log transform was used for de-clustering the distribution of SUV values. Finally, ε_{ij} is measurement error, assumed to have a random Gaussian distribution with zero mean and SD log(S_{ij}) σ_e. The increase of the error variance was modeled to reflect the observed residuals and is typical behavior for image intensity measurements, which approximate Poisson statistics. Model (1) was fit by the method of restricted maximum likelihood (REML) using the nlme package in the R computing platform (www.r-project.org).

Results

Standardized uptake values (SUV_{mean}) and (SUV_{max}) for all regions are shown in **Tables 1** and **2**, respectively. For regions with modest to high uptake (non-TOF SUV_{mean}>2) significantly higher values for SUV_{mean} were seen in normal trabecular bone (femoral head, ribs, and T12), cortical bone (femoral cortex), and abnormal osseous regions including both degenerative joint disease and metastatic lesions compared to non-TOF reconstructions ($p \leq 0.0001$ for all regions). The very low background regions (non-TOF $SUV_{mean} \leq 0.65$) showed slightly lower mean values in liver, fat, and brain in TOF compared to conventional non-TOF reconstructions ($p<0.0001$ for all regions). The SUV_{mean} in the paraspinal muscles and aorta showed a trend towards lower values in TOF compared to non-TOF values, but these were not statistically significant when corrected for multiple comparisons (p=0.0065 and 0.0056, respectively).

The differences in SUV_{mean} are expressed as both relative percentages of non-TOF values, and as absolute SUV_{mean} differences as summarized in **Table 3**. The mean differences in SUV_{mean} for soft tissues was only slightly lower (-0.15, -0.02, -0.06 for liver, adipose, and brain, respectively) for TOF compared to non-TOF. The mean differences in SUV_{mean} for osseous structures were only slightly higher (0.09, 0.10, 0.16, 0.36, 0.18 for T12, femoral cortex, femoral head, and rib, respectively) in TOF compared to non-TOF. Similarly, the mean difference in SUV_{mean} in degenerative joint disease was 0.36 (approximately 3.7%) higher, and in metastases was 0.18 (approximately 2.5%) higher for TOF compared to non-TOF.

For difference in SUV_{max}, the TOF values showed changes in the same direction compared to the above analysis for SUV_{mean} (**Table 2**); however, some osseous regions did not show a statistically significant difference (T12, femoral cortex, rib, or metastatic lesions). For soft tissue background with low uptake, the SUV_{max} also showed changes in the same direction as the above SUV_{mean}; the liver, adipose, brain, and aortashowed slightly lower SUV_{max} in TOF compared to non-TOF reconstructions (**Table 3**).

The correlations of TOF versus non-TOF were very high for the osseous structures. For soft tissues with very low uptake, the TOF versus non-TOF comparisons showed correlation coefficients that were generally lower (**Figure 2**; $R^2<0.9$) compared to normal osseous structures (**Figure 3**; $R^2>0.9$), benign degenerative changes (**Figure 4**; $R^2>0.9$), and metastatic lesions (**Figure 5**; $R^2>0.9$).

The analysis of the influence of the scan variables (tumor location, tumor volume, patient weight, and metastatic lesion SUV_{mean}) is shown in **Table 4**. Based on the multivariate analysis model, the estimated mean difference in SUV_{mean} was 0.22 for TOF based measurements as opposed to non-TOF measurements

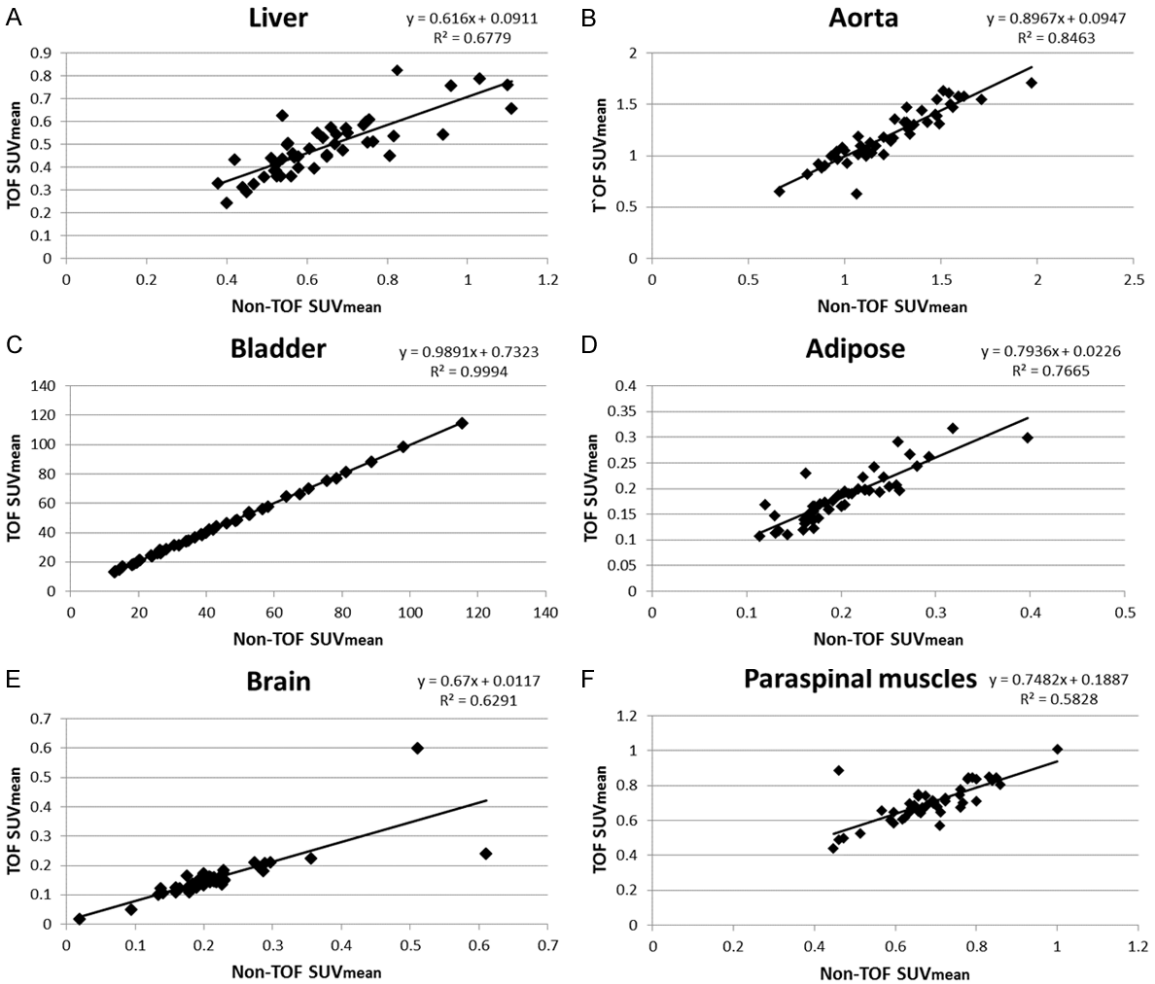

Figure 2. Normal non-osseous SUV_{mean} correlations: TOF versus non-TOF. (A) liver, (B) aorta, (C) bladder, (D) adipose, (E) brain, and (F) paraspinal muscle.

if a 2.5 cm^3 size metastatic lesion was in a rib. This supports the hypothesis that the differences in TOF SUV_{mean} due to contrast recovery are relatively greater in the smaller lesions as shown in (**Figure 6**). This difference was only correlated with the rib as a site specific change. This is consistent with the hypothesis that rib lesions are more commonly small and more likely to show a relationship to differences in SUV_{mean} than lesions in other locations which may have a wider variability in size. There is a highly significant decrease in the difference in SUV_{mean} as size of lesion increases: on average the difference decreases by 0.14 for every cm^3 increase in lesion size. This suggests that there will be no significant difference in SUV mean between TOF and non-TOF based measurements for a lesion sized more than 4 cm^3. There was also a marginally significant effect of the SUV_{mean} of the metastatic lesion, in that the difference between TOF and non-TOF based measurements was smaller by 0.16 for every unit increase in the mean SUV of the lesion. This is also consistent with the general principle that smaller lesions will be associated with lower SUV_{mean} due to the partial volume effect. Finally, there was no significant effect of body weight.

To assess the image noise of TOF and non-TOF reconstructions, the standard deviation of the background was measured. The standard deviations for the background regions of paraspinal muscles and adipose are quite comparable, and only slightly lower in TOF reconstructions. Again, although statistically significant, the magnitude of the differences is very small as shown in **Table 5**, supporting the clinical

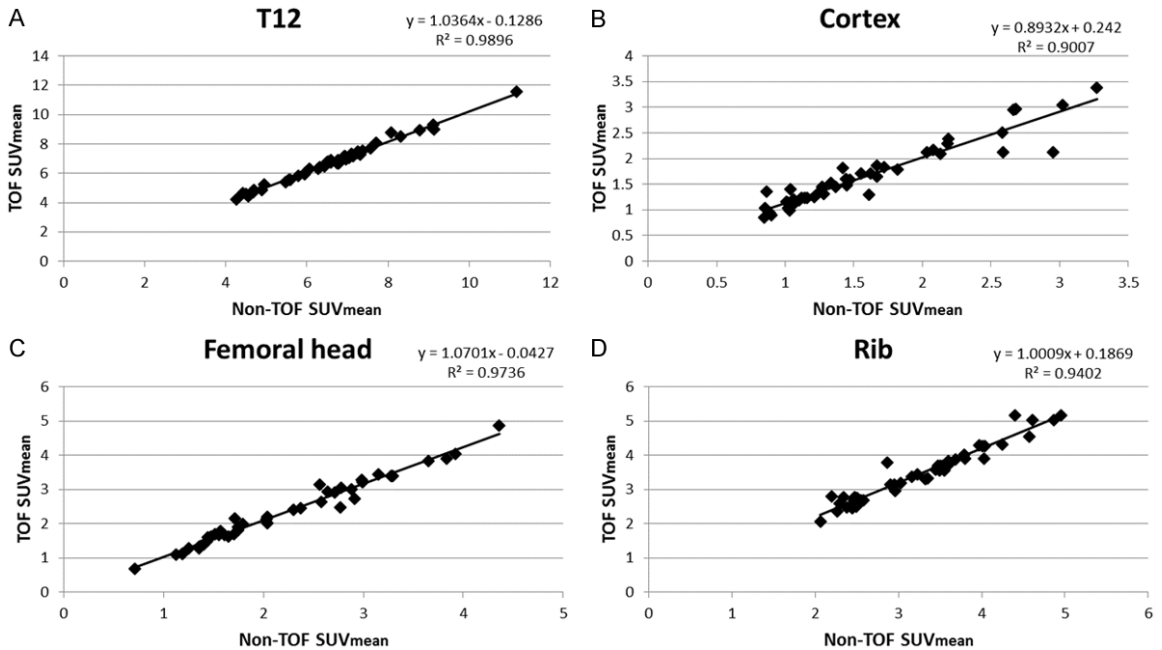

Figure 3. SUV_{mean} of normal osseous structures: TOV versus non-TOF. (A) T12, (B) femoral cortex, (C) femoral head, and (D) rib.

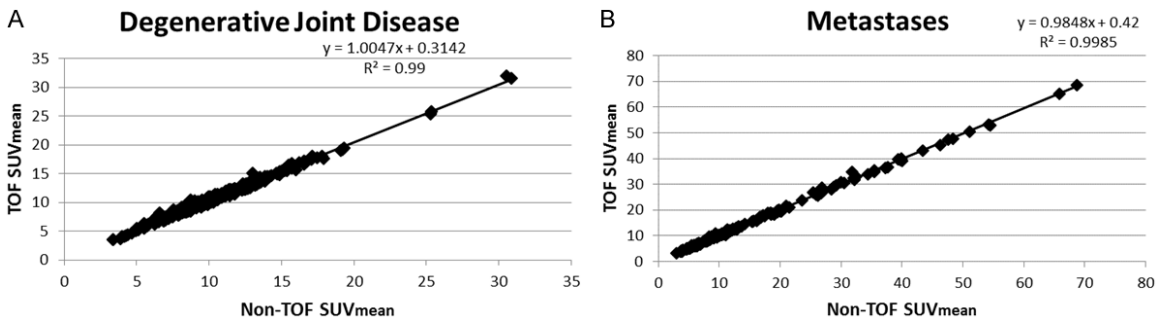

Figure 4. SUV_{mean} of TOF versus non-TOF for (A) degenerative joint disease, (B) metastases.

impression of approximately equivalent noise level of TOF and non-TOF reconstructions.

Discussion

The TOF reconstruction improvements in FDG PET/CT quantification have been described as improved contrast recovery at a given noise level. Although phantom studies and preliminary patient studies with FDG PET have been reported, the quantitative effects of TOF reconstructions of clinical [18F] NaF PET/CT may be different due to differences in radiotracer uptake and biodistribution.

In phantom studies, improved contrast recovery from TOF results in quantitatively more accurate measurements that are closer to the actual activities, particularly for smaller regions due to the partial volume effect [5]. Compared to non-TOF reconstructions, the TOF lesions with no activity ("cold" lesions) are quantitatively lower, and lesions with high activity ("hot" lesions) are quantitatively higher due to improved spatial resolution. In patient studies, improved contrast recovery from TOF is expected to increase SUV_{mean} measurements in small structures with high uptake.

Our results demonstrated significantly higher SUV_{mean} activity in TOF compared to non-TOF reconstructions in osseous structures. This was most apparent in small osseous lesions, concordant with the expectation of improved

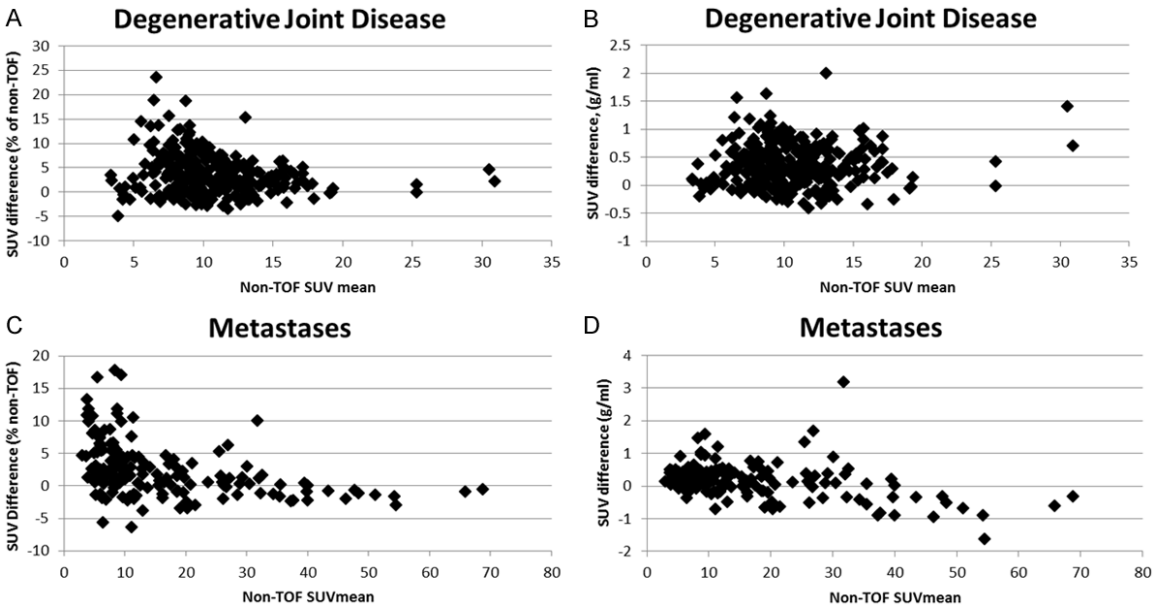

Figure 5. Difference in SUV_{mean} TOF versus non-TOF. (A) DJD expressed as % of non-TOF, (B) DJD expressed in absolute SUV units, (C) metastatic lesions SUV expressed as % of non-TOF, and (D) metastatic lesions expressed in absolute SUV units.

Table 4. Fitted multivariate linear mixed model of differences in SUV_{mean} for metastatic lesions

	Value	Std. Error	t-value	*p*-value
Baseline mean (Rib)	0.22	0.10	2.13	0.04
Clavicle	-0.31	0.62	-0.50	0.62
Femur	0.15	0.21	0.69	0.49
Humerus	0.14	0.24	0.59	0.55
Other	0.31	0.31	1.00	0.32
Pelvis	-0.05	0.10	-0.51	0.61
Scapula	-0.07	0.14	-0.49	0.63
Skull	-0.06	0.17	-0.38	0.71
Spine	-0.01	0.11	-0.08	0.94
Sternum	-0.25	0.23	-1.07	0.28
log (Volume)	-0.14	0.05	-2.98	0.004
Weight	0.005	0.01	0.97	0.34
log (SUV mean)	-0.16	0.07	-2.14	0.03

contrast recovery for small objects. Although a significantly higher SUV_{mean} measurement was seen in TOF reconstructions for osseous structures overall, the average magnitude of the difference was relatively modest. Normal soft tissues with very low [18F] NaF PET uptake showed slightly lower SUV_{mean} with TOF compared to non-TOF reconstructions. Again, this is consistent with improved contrast recovery from TOF.

For metastatic lesions, the lesion size was highly significant as a variable associated with differences in SUV_{mean} between TOF and non-TOF measurements, as expected due to a greater influence of improved contrast recovery in smaller lesions. Rib lesions, which are typically small, also showed a correlation with differences in SUV_{mean}, but other lesion locations did not. Not surprisingly, the SUV_{mean}, which is highly influenced by the contrast recovery in small lesions, also showed a correlation with quantitative differences in SUV_{mean} between TOF and non-TOF measurements.

Patients with a large body habitus could potentially gain contrast improvement through reduced background scatter, however, our data did not show significant correlation between patient weight and SUV_{mean} in metastatic lesions. Although patient weight is expected to correlate with patient transaxial diameter, and could improve SUV_{mean} with better activity localization from TOF, this effect was not apparent in our sample population. This raises the possibility that the normally very high uptake of NaF in bone and very low uptake in soft tissues (i.e. relatively low scatter fraction contribution) did not significantly benefit from improved quantitative accuracy using TOF capability. Another potential explanation is that this effect is very small and not detectable with our sample size.

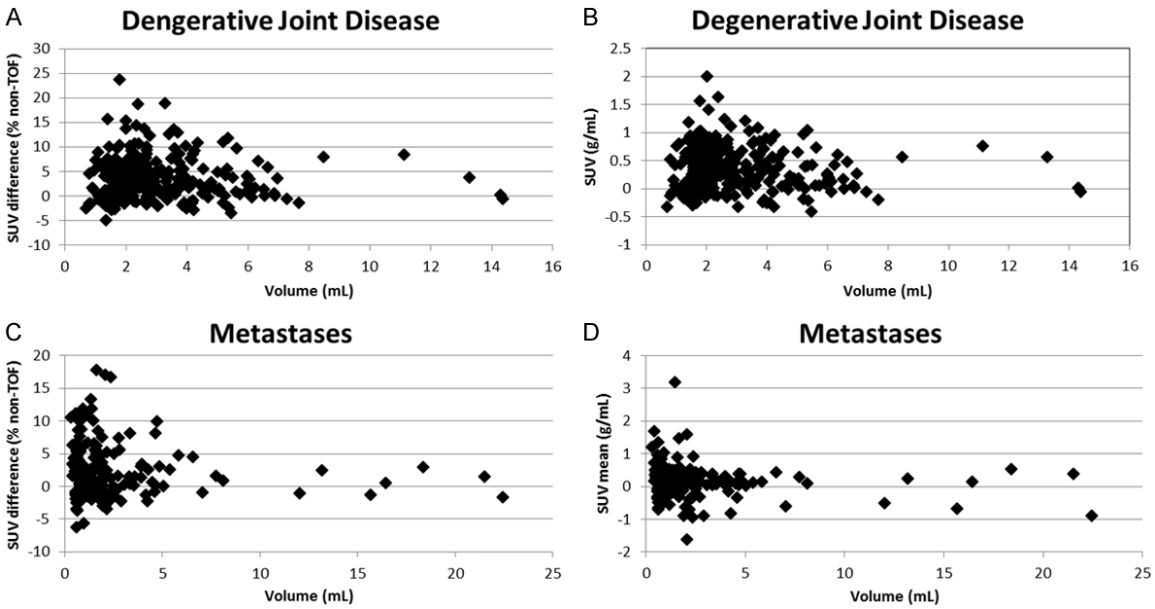

Figure 6. Relationship of lesion volume to difference in SUV_{mean}. (A) DJD difference expressed as % difference = (TOF-non-TOF)/non-TOF * 100%), (B) DJD difference expressed in absolute SUV_{mean} units (TOF-non TOF), and (C) metastatic lesion difference expressed as % difference = (TOF-non-TOF)/non-TOF * 100%), (D) metastatic lesion difference expressed in absolute SUV_{mean} units (TOF-non TOF).

Table 5. Average STD for SUV_{mean} of the paraspinal muscles and fat: TOF versus non-TOF

Organ	TOF STD (mean ± STD)	Non-TOF STD (mean ± STD)	*p*-value (paired t-test)
Paraspinal muscle	0.1318±0.0347	0.1414±0.0363	.0006
Fat	0.0469±0.0147	0.0532±0.155	<0.0001

Further investigation in a larger sample size would be needed for confirmation.

This study has several limitations. First, due to the retrospective design, the clinical [18F] NaF PET/CT scans were all obtained in adult male patients for staging of prostate cancer. A larger study would perhaps be needed to generalize these findings for a larger population (e.g. a wider range of patient weights). Second, this retrospective study did not address the clinical relevance of these quantitative differences, and thus, a subsequent study with correlation of imaging parameters with patient outcomes would be desirable. This data, however, provides a useful estimation of the variability to facilitate the planning such a prospective study. Third, the PET acquisition and reconstruction parameters used in this study were not rigorously optimized. The iterations chosen for the reconstructions were those used in our clinical practice. This set of reconstruction iterations were chosen to slightly improve noise as confirmed in **Table 5**; however, these parameters simultaneously provided a clinically detectable improvement in contrast recovery for TOF SUV_{mean} measurements in bone and background tissues. These findings support the adequacy of theseclinical iterative reconstruction parameters.

Summary

At a given reconstruction image noise level, TOF reconstructions provide higher contrast recovery. For clinical [18F] NaF PET/CT, our results demonstrate values of SUV_{mean} that are slightly higher compared to non-TOF for normal osseous structures, as well as for benign and malignant bone lesions. TOF SUV_{mean} is also slightly lower than non-TOF SUV_{mean} in soft tissue regions with very low [18F] NaF uptake such as adipose tissue, brain and liver. The overall effect of TOF is to produce high contrast bone to background soft tissue ratios. Although the differences in quantification are statistically significant, the average magnitudes of the differences are relatively modest. Because

improved contrast recovery from TOF has a greater quantitative effect on smaller lesions, early osseous metastatic lesions could potentially show higher SUV measurements. This suggests that improved contrast from TOF could positively impact the early detection of metastatic disease and improve lesion quantification for [18F] NaF PET/CT. These differences in TOF vs. non-TOF [18F] NaF PET/CT should be considered when evaluating response to therapy and in the design of multi-center clinical trials.

Acknowledgements

We gratefully acknowledge the assistance of Robin Davis in assisting with anonymization of the data.

Disclosure of conflict of interest

None.

Address Correspondence to: Dr. Bennett B Chin, Department of Radiology, Division of Nuclear Medicine, DUMC Box 3808, Durham, NC 27710, USA. Tel: 919-684-7698, Fax: 919-684-7135. E-mail: chin0004@dm.duke.edu

References

[1] Even-Sapir E, Metser U, Flusser G, Zuriel L, Kollender Y, Lerman H, Lievshitz G, Ron I, Mishani E. Assessment of malignant skeletal disease: initial experience with [18F]-fluoride PET/CT and comparison between [18F]-fluoride PET and [18F]-fluoride PET/CT. J Nucl Med 2004; 45: 272–278.

[2] Iagaru A, Mittra E, Dick DW, Gambhir SS. Prospective evaluation of (99m)Tc MDP scintigraphy, (18)F NaF PET/CT, and (18)F FDG PET/CT for detection of skeletal metastases. Mol Imaging Biol 2012; 14: 252-9.

[3] Even-Sapir E, Metser U, Mishani E, Lievshitz G, Lerman H, Leibovitch I. The detection of bone metastases in patients with high-risk prostate cancer: 99mTc-MDP Planar bone scintigraphy, single- and multi-field-of-view SPECT, 18F-fluoride PET, and 18F-fluoride PET/CT. J Nucl Med 2006; 47: 287-97.

[4] Scher HI, Halabi S, Tannock I, Morris M, Sternberg CN, Carducci MA, Eisenberger MA, Higano C, Bubley GJ, Dreicer R, Petrylak D, Kantoff P, Basch E, Kelly WK, Figg WD, Small EJ, Beer TM, Wilding G, Martin A, Hussain M. Design and end points of clinical trials for patients with progressive prostate cancer and castrate levels of testosterone: recommendations of the Prostate Cancer Clinical Trials Working Group. J Clin Oncol 2008; 26: 1148-1159.

[5] Karp JS, Surti S, Daube-Witherspoon ME, Muehllehner G. Benefit of time-of-flight in PET: experimental and clinical results. J Nucl Med 2008; 49: 462-70.

[6] Surti S, Karp JS, Popescu LM, Daube-Witherspoon ME, Werner M. Investigation of time-of-flight benefit for fully 3-D PET. IEEE Trans Med Imaging 2006; 25: 529-38.

[7] Surti S, Scheuermann J, El Fakhri G, Daube-Witherspoon ME, Lim R, Abi-Hatem N, Moussallem E, Benard F, Mankoff D, Karp JS. Impact of time-of-flight PET on whole-body oncologic studies: a human observer lesion detection and localization study. J Nucl Med 2011; 52: 712-9.

[8] El Fakhri G, Surti S, Trott CM, Scheuermann J, Karp JS. Improvement in lesion detection with whole-body oncologic time-of-flight PET. J Nucl Med 2011; 52: 347-53.

[9] Akamatsu G, Mitsumoto K, Taniguchi T, Baba S, Sasaki M. Influences of point-spread function and time-of-flight reconstructions on standardized uptake value of lymph node metastases in FDG-PET. Eur J Radiol 2014; 83: 226-230.

[10] Prieto E, Domínguez-Prado I, García-Velloso MJ, Peñuelas I, Richter JÁ, Martí-Climent JM. Impact of time-of-flight and point-spread-function in SUV quantification for oncological PET. ClinNucl Med 2013; 38:103-9.

[11] Lois C, Jakoby BW, Long MJ, Hubner KF, Barker DW, Casey ME, Conti M, Panin VY, Kadrmas DJ, Townsend DW. An assessment of the impact of incorporating time-of-flight information into clinical PET/CT imaging. J Nucl Med 2010; 51: 237-245.

[12] Oldan J, Chisholm K, Kurdziel K, Wilson J, Chin BB. Sodium fluoride PET/CT of metastatic disease burden: Preliminary results of reproducibility measurements. J Nucl Med 2013; 54 Supplement 2: 1433.

[13] Wilson JM, Turkington TG. TOF-PET Small lesion image quality measured over a range of phantom sizes. IEEE Trans NuclSci 2013; 60: 1589-1595.

[14] Chen W, Dilsizian V. Targeted PET/CT imaging of vulnerable atherosclerotic plaques: microcalcification with sodium fluoride and inflammation with fluorodeoxyglucose. Curr Cardiol Rep 2013; 15: 364.

[15] Dweck MR, Chow MW, Joshi NV, Williams MC, Jones C, Fletcher AM, Richardson H, White A, McKillop G, van Beek EJ, Boon NA, Rudd JH, Newby DE. Coronary arterial [18F]-sodium fluoride uptake: a novel marker of plaque biology. J Am Coll Cardiol 2012; 59: 1539-48.

[16] Chen CH, Muzic RF Jr, Nelson AD, Adler LP. Simultaneous recovery of size and radioactivity concentration of small spheroids with PET data. J Nucl Med 1999; 40: 118-130.

[17] Akkas BE, Demirel BB, Dizman A, Vural GU. Do clinical characteristics and metabolic markers detected on positron emission tomography/computerized tomography associate with persistent disease in patients with in-operable cervical cancer? Ann Nucl Med 2013; 27:7 56-763.

[18] Usmanij EA, de Geus-Oei LF, Troost EG, Peters-Bax L, van der Heijden EH, Kaanders JH, Oyen WJ, Schuurbiers OC, Bussink J. 18F-FDG PET early response evaluation of locally advanced non-small cell lung cancer treated with concomitant chemoradiotherapy. J Nucl Med 2013; 54: 1528-34.

[19] Boktor RR, Walker G, Stacey R, Gledhill S, Pitman AG. Reference range for intrapatient variability in blood-pool and liver SUV for [18F]-FDG PET. J Nucl Med 2013; 54: 677-682.

[20] de Langen AJ, Vincent A, Velasquez LM, van Tinteren H, Boellaard R, Shankar LK, Boers M, Smit EF, Stroobants S, Weber WA, Hoekstra OS. Repeatability of 18F-FDG uptake measurements in tumors: a metaanalysis. J Nucl Med 2012; 53: 701-8.